Low-temperature crystal structure and magnetic properties of Gd_{5}Ge_{3}

Ya. Mudryk, D. Paudyal, V. K. Pecharsky, and K. A. Gschneidner, Jr.

Phys. Rev. B **85**, 014116 — Published 27 January 2012

DOI: 10.1103/PhysRevB.85.014116

Low Temperature Crystal Structure and Magnetic Properties of Gd_5Ge_3

Ya. Mudryk[a], D. Paudyal

The Ames Laboratory of U.S. Department of Energy, Iowa State University, Ames, Iowa 50011-3020, USA

V. K. Pecharsky and K. A. Gschneidner, Jr.

The Ames Laboratory of U.S. Department of Energy, Iowa State University, Ames, Iowa 50011-3020, USA and

Department of Materials Science and Engineering, Iowa State University, Ames, Iowa 50011-2300, USA

The Gd_5Ge_3 compound prepared using high purity gadolinium undergoes a structural deformation from hexagonal Mn_5Si_3-type structure into a new orthorhombic crystal structure. The temperature of the structural transition coincides with the Neél temperature (T_N), confirming the coupling between magnetism and crystal structure. The same intermetallic compound prepared using a commercial grade of gadolinium shows only a minor orthorhombic structural deformation at T_N, which is 19 K lower than that of a Gd_5Ge_3 sample prepared from the high purity Gd. The first principles electronic structure calculations confirm the antiferromagnetic orthorhombic structure as the ground state of Gd_5Ge_3, and show that interstitial impurities affect the strength of the antiferromagnetic interactions.

[a] corresponding author: slavkomk@ameslab.gov

PACS: 61.50.Ks, 71.20.Eh, 75.30.-m

INTRODUCTION

The well known, but somewhat unfortunate, peculiarity of solid state science is that the most interesting and richest phenomenology is often observed at cryogenic temperatures. Yet, practical applications of many of the observed low temperature effects persistently reach into everyday life – the use of superconducting magnets in the magnetic resonance imaging (MRI) diagnostics is only one of numerous examples. Therefore, the studies of low temperature properties of materials are equally important both for the fundamental and applied science. Knowledge of the low temperature crystal structure of the material, which may be different from its room temperature structure, is often a critical requirement for the successful interpretation of the measured physical properties. For example, first principles calculations are usually performed for the "T = 0 K" state requiring the knowledge of the crystal structure at temperatures as low as possibly achievable.

The rare earth based compounds attract constant attention because of rich physics. For example, the R_5T_4 family of compounds[1,2] (where R is a rare earth metal, and T is Group 14 element) shows a unique combination of magnetostrictive,[3,4] magnetoresistive,[5-7] and magnetocaloric[8-10] properties as well as a series of other interesting physical phenomena, such as spontaneous generation of voltage,[11,12] kinetic arrest,[13] and magnetic deflagration.[14] These effects are related to the fact that crystallographic and magnetic lattices in these compounds are often coupled, undergoing concomitant transitions that can be controlled by chemical composition, temperature, pressure, and/or magnetic field.[15] The $Gd_5Si_xGe_{4-x}$ pseudobinary system[16] has become a well recognized model

system for the investigation of the typically elusive composition-structure-property relationships in intermetallic materials.[17,18]

The Gd_5Ge_3 phase and its solid solution compounds $Gd_5Si_xGe_{3-x}$ have been commonly observed in the Gd_5Ge_4 and $Gd_5Si_xGe_{4-x}$ alloys as a minor impurity that forms a peculiar plate-like microstructure.[19,20] The role of $Gd_5Si_xGe_{3-x}$ platelets in the initiation of the paramagnetic-ferromagnetic phase transition in $Gd_5Si_2Ge_2$ has recently been studied.[21] Little, however, is known about the structure – physical property relationships of the 5:3 compounds in general, and the parent germanide Gd_5Ge_3 in particular despite a fair number of publications that report on various aspects of structure and physical properties of the binary germanide.

Two studies on the formation of the Gd_5Ge_3 compound were published independently in 1964, and both reported the Mn_5Si_3 type of crystal structure for this compound.[22,23] This compound adopts space group symmetry $P6_3/mcm$, and its unit cell encompasses three independent atomic positions, two of which (4*d* and 6*g*) are occupied by the Gd atoms, and one position (6*g*) is occupied by Ge. A few years later the Mn_5Si_3 type structure was confirmed,[24,25] and the basic magnetic properties of Gd_5Ge_3 and other R_5Ge_3 germanides were reported by Buschow and Fast.[24] The paramagnetic (PM) to antiferromagnetic (AFM) transition of Gd_5Ge_3 was observed at 48 K.[24] Narasimhan *et al.*[26] performed magnetic susceptibility measurements on several R_5Ge_3 and R_5Si_3 compounds but they did not report the transition temperature for Gd_5Ge_3. Later measurements of the linear thermal expansion (LTE),[27] magnetic,[28] and electrical resistivity[28] properties report a

much higher Neél temperature (T_N) of 68 K. The LTE measurements performed on the polycrystalline sample showed that the anomaly in lattice dimensions coincides with the magnetic transition,[27] but the authors suggested the second order nature of this transformation. Heat capacity measurements[29] performed on a polycrystalline alloy reported the main transition around 77 K (which is by ~30 and ~10 K higher than earlier reports) and another heat capacity anomaly at 195 K. Magnetization measurements performed by Canepa *et al.*[30] indicated T_N of 74 K. At the same time the paramagnetic Weiss temperature (θ_p) is positive and large, as reported by Narasimhan *et al.*[26] (54.8 K) or by Canepa *et al.*[30] (65 K), indicating substantial ferromagnetic coupling in the ground state of magnetic sublattice of the compound. It is interesting to note significant discrepancies in the value of T_N reported in different sources (generally, more recent papers report higher T_N). The highest T_N = 80 K for the Gd_5Ge_3 compound was reported by Dhar *et al.*[31] Same authors observed another magnetic transition near 50 K. As we will see later, it is important to note that the lattice parameters and unit cell volume of Gd_5Ge_3 measured in this paper[31] are also the highest among all those previously reported.[24,25,27,28]

Recently, a number of magnetic, electrical transport, neutron and x-ray diffraction measurements have been performed using single crystals of Gd_5Ge_3.[32-34] Two magnetic transitions were reported: T_N at 76 K, and a spin reorientation transition at T = 52 K. The magnetic properties of single crystalline Gd_5Ge_3 are anisotropic reflecting the hexagonal crystal structure. There is, however, a significant discrepancy between the properties of the single crystals reported in references 32 and 33. The magnetization (M) measured as a function of field shows linear increase of M with applied magnetic field H both along the

c-axis and in the *ab*-plane at 4.2 K.[32] However, the same measurements performed on a different Gd_5Ge_3 single crystal[33] show a metamagnetic-like transition when the data were collected along the *a*-axis, while the data collected along the *c* direction are essentially the same as reported in Ref. 32. The x-ray diffraction analysis of the (550) and (008) Bragg reflections revealed strong anisotropic magnetostriction, namely the expansion of the lattice along the *a*-axis and contraction along the *c*-axis, which occurs above 4 kOe at 4.2 K.[33] An absence of any distortion affecting symmetry was claimed in this work, since the full width at half maximum of the examined Bragg reflections remained constant during magnetic field changes.[33] The discrepancy between two studies was explained by the better quality of the single crystal in Ref. 33 compared to the same of Ref. 32.

The most recent study of the Gd_5Ge_3 single crystal employed both neutron diffraction and dilatometry measurements to determine the changes in the lattice as a function of both temperature and magnetic field.[34] The anomalies in lattice dimensions were observed at T_N during cooling and heating in zero field, namely expansion along the hexagonal (*c*) axis and contraction in the hexagonal (*ab*) plane. With the application of magnetic field the sample shrinks along the *a* direction by -300 ppm and expands along the *c* direction by 900 ppm. The magnetostriction is irreversible at 5 K, shows hysteresis at 20 K, and is not observed at 100 K, i.e. above T_N.[34] Interestingly, the authors report that the propagation vectors determined using neutron diffraction for two different Gd_5Ge_3 samples are different [(0 0 0.4) and (0.3 0.3 0)] while T_N = 76 K remains the same.

The analysis of the available literature discussed above leads to a conclusion that the Gd_5Ge_3 compound has a rich physics, which however, is far from being clearly understood. The magnetostriction observed in this compound and the strong sample dependence of its basic physical properties call for a closer look into the intriguing behavior of the crystal lattice of Gd_5Ge_3 and its expected coupling with the magnetic sublattice. Here we report a study of the physical properties and crystal structure of two polycrystalline Gd_5Ge_3 alloys made from the starting materials of different purity. The first principles calculations of the electronic structure of Gd_5Ge_3 are used to interpret and partially explain the experimental findings.

EXPERIMENTAL TECHNIQUES

The first set of Gd_5Ge_3 samples for the experiments (henceforth samples A, A-HT, and B) were polycrystalline alloys arc-melted from the elements in an Ar atmosphere using high purity Gd metal prepared by the Materials Preparation Center at the Ames Laboratory of U.S. Department of Energy.[35] The Gd was at least 99.7 at. % pure with respect to *all* elements in the Periodic Table (the major impurity is oxygen: 2375 at. ppm). In order to verify the suggestion that the value of T_N in Gd_5Ge_3 is strongly affected by the purity of the rare earth metal used in sample preparation, three additional samples have been prepared using commercial grade Gd, purity of which is generally quoted at 99.9 % (probably wt. % and not at. %), but is typically on the order of 90-95 at.%[36,37]. The elemental Ge for sample preparation was purchased from Meldfom Ltd. (at least

99.99 wt. % pure). The compositions of the samples prepared using commercial Gadolinium were: Gd_5Ge_3 (sample C), $Gd_{5.02}Ge_3$ (sample D), and $Gd_{5.1}Ge_3$ (sample E).

According to room temperature X-ray powder diffraction measurements, all samples appear as single phase materials with the Mn_5Si_3-type crystal structure (space group $P6_3/mcm$). A part of sample A was heat treated at 850 °C for 1 week (sample A-HT). The heat treated sample was also a single phase material and this sample (A-HT) was primarily used in magnetization, heat capacity, and temperature dependent X-ray powder diffraction measurements. The SEM analysis of samples A-HT and C confirms that both samples are primarily single phase materials containing a small (~0.5 vol.%) fraction of linear features similar to those previously observed in the R_5T_4 series of alloys.[19,20] The full results of the ongoing miscrostructural investigation of these alloys will be published elsewhere when available. The lattice parameters of the prepared samples are listed in Table 1. Chemical analysis of the Gd_5Ge_3 compounds prepared from the materials of different purity (samples A and C) was performed to analyze for oxygen, nitrogen, and carbon content (Table 2). In addition, two samples with nominal stoichiometry $Gd_{11}Ge_{10}$ and Gd_3Ge were prepared from Ames Laboratory high purity Gd in order to check the existence of these compounds, and if they exist, to examine their magnetic properties. Both samples were found to be multiphase alloys containing only the known phases in agreement with the Gd-Ge phase diagram.[38]

The temperature dependencies of dc magnetization and ac magnetic susceptibility of bulk polycrystalline samples were studied using Quantum Design Superconducting Quantum

Interference Device (SQUID) magnetometer, model MPMS XL-7. The isothermal magnetization was measured at 5 and 20 K in magnetic fields ranging from 0 to 140 kOe in the Quantum Design Physical Property Measurement System (PPMS) by using the Vibrating Sample Magnetometer (VSM) option. The pressure dependence of magnetization was studied by using a commercial HMD High Pressure Cell designed for use in the Quantum Design MPMS SQUID magnetometers. The heat capacity was measured using a semi-adiabatic heat pulse calorimeter[39] in magnetic fields from 0 to 75 kOe. The temperature and magnetic field dependent x-ray powder diffraction measurements were performed using the Gd_5Ge_3 powder (particle size <25 μm, mixed with GE varnish) at temperatures ranging from 5 to 300 K and in magnetic fields between 0 and 40 kOe. The details of the sample preparation and experimental setup can be found in Ref. 40.

EXPERIMENTAL RESULTS

Magnetic Properties

The magnetization of the polycrystalline Gd_5Ge_3 (sample A-HT) measured as a function of temperature at constant magnetic field [$M(T)$] is shown in Fig. 1. In 1 kOe the PM to AFM transition is observed at T_N = 87 K (T_N here is defined at a maximum magnetization value on the $M(T)$ curve) and two additional, possibly spin reorientation (SR), transitions are seen at T_{SR1} = 44 K and at T_{SR2} = 68 K (Fig. 1). The Neél temperature shows very weak magnetic field dependence, while the spin reorientation transitions notably shift to

lower temperatures at higher magnetic fields (Fig. 1a). In addition to these transitions, the ZFC (zero field cooled heating) data collected at 70 kOe show two anomalies at 10 and 24 K (Fig. 1a). These anomalies are likely related to additional spin reorientation processes indicating complex magnetic structure of Gd_5Ge_3. There is a small hysteresis between ZFC heating and field cooled cooling (FCC) data below T_{SR1}. The appearance of this hysteresis does not necessary indicate a first order transition and is rather typical for the domain wall motion activation. However, it occurs even in strong magnetic fields, and in view of strong magnetostriction observed in Gd_5Ge_3 single crystal,[33] the possibility of at least partially structural origin of this hysteresis should be considered.

The *ac* magnetic susceptibility measurements of the as cast Gd_5Ge_3 (A) revealed the presence of the unreacted Gd metal in the sample (Fig. 2), which orders ferromagnetically at 293 K. At the same time, the heat treated sample A-HT does not contain Gd. However, the *ac* susceptibility indicates another transition at ~195 K in both as cast and heat treated samples (Fig. 2) in addition to the AFM and SR transitions. Note that the T_N is essentially the same for both the as cast and heat-treated samples, so the annealing is not a factor affecting the ordering temperature as it was suggested by Dhar *et al*.[31] Clearly, the strength of the signal that corresponds to the transition at ~195 K drastically decreases after the heat treatment and the signal from the Gd metal completely disappeared. This indicates that the 195 K transition belongs to a magnetic impurity phase, in addition to Gd, which should be a phase that is richer in Ge than Gd_5Ge_3. Neither Gd_5Ge_4 nor GdGe have magnetic ordering transitions at ~195 K and the $M(T)$ curves of the prepared neighboring alloys (not shown), $Gd_{11}Ge_{10}$ and Gd_3Ge, did not

show this transition as well. Further, as follows from both X-ray powder diffraction and scanning electron microscopy data, sample A has no impurities other than the observed linear features. Even though the nature of the linear features is not clear, it is reasonable to assume that they are the cause of this magnetic transition. One feasible explanation is that the composition of the linear features here is different from those observed in R_5T_4 alloys. In addition, stresses at grain boundaries that form in a polycrystalline sample due to rapid cooling from a melt may create effects similar to high non-hydrostatic pressure raising the ordering temperature of this impurity. If this is the case, than the strain relief during the heat treatment should lead to a weaker signature of the transition at 195 K as is observed experimentally (see Fig. 2).

The isothermal magnetization data (Fig. 3) show a weak spin reorientation transition that slightly increases the sample's magnetization around 70 kOe but does not result in a ferromagnetic state. Hysteresis is observed around this transition at 5 K but it almost disappears at 20 K. Even at fields as high as 140 kOe, the material remains essentially antiferromagnetic, and no sharp metamagnetic transitions like the one observed along the *a*-axis in Ref.33 occur in our measurements. The presence of hysteresis indicates that the magnetic and crystalline sublattices remain coupled.

The *M*(T) dependences of the A-HT sample were collected using high-pressure cell at normal pressure, and at 0.1 and 0.6 GPA in 1 kOe dc magnetic field during cooling from 150 to 2 K. The results are shown in Fig. 4. The application of an external pressure slightly increases the antiferromagnetic ordering temperature of the Gd_5Ge_3 by

~3 K/GPA (or ~0.3 K/kbar). This change agrees with the fact that the unit cell volume of the low temperature antiferromagnetic phase (see the *Crystal Structure* section below) is slightly smaller than the unit cell volume of the paramagnetic phase.

Heat Capacity

Heat capacity of the Gd_5Ge_3 compound was measured in 0, 20, 50, and 75 kOe (Fig. 5). The heat capacity data basically agree with the magnetization data – the main transition at ~83 K is accompanied by two weaker transitions at approximately 45 K and 70 K. The third transition appears in 75 kOe field at ~28 K and it agrees with the M(T) data collected at 70 kOe. A weak magnetic transition observed at ~ 10 K in the 70 kOe M(T) data is not seen in the heat capacity data. The heat capacity behavior at T_N suggests the transition is of first order contrary to what was suggested in earlier studies[27,34] as the transition remains relatively sharp even in high magnetic fields. In the previous papers[27,34] the conclusion that the Gd_5Ge_3 undergoes the second order phase transition at its Neél temperature was based on the results of the LTE experiments as no hysteresis or sharp changes in the sample dimensions have been observed. The heat capacity study of Gd_5Ge_3[29] reports the strong thermal effect at T_N, but the authors of this earlier work do not comment about the thermodynamic nature of the transition. Apparently, the first order character of this AFM - PM transition is weak; there is no hysteresis around T_N in the magnetization data and the volume difference between the high- and low-temperature phases (see below) is small.

Crystal Structure

During cooling in the absence of magnetic field the Gd_5Ge_3 sample shows nearly linear lattice contraction from 300 K to the magnetic ordering temperature 85 K (Fig. 6). No anomaly was observed around 195 K in agreement with the heat capacity data (Fig. 5). Below 80 K the x-ray powder diffraction patterns of Gd_5Ge_3 clearly indicate a structural distortion, as most of the Bragg peaks become wider and some split indicating lower crystallographic symmetry. A detailed crystallographic analysis was performed using the x-ray powder diffraction pattern collected at 20 K (Fig. 7). The largest splitting occurs for the (*hk*0) and (*h*00) reflections while a few resolved (00*l*) peaks remain unaffected by the transition. Assuming that the new crystal structure must be closely related to the parent Mn_5Si_3-type structure several isomorphic orthorhombic space groups were chosen for the preliminary indexing. It was found that the x-ray pattern can be successfully indexed using *Cmcm* space group. The atomic positions were then generated using International Tables for Crystallography,[41] and the final result was obtained using the Rietveld refinement (LHPM Rietica[42]). The lattice parameters and atomic positions of the orthorhombic Gd_5Ge_3 compound at 20 K, which essentially represents a new structure type, are listed in Table 3. From the temperature dependence of the lattice parameters shown in Fig. 6, it is clear that the distortion occurs in the *ab* plane, similar to pure Gd. Nearly identical results were obtained during the heating, which was performed from 5 to 120 K. We cannot either definitely confirm or disprove the presence of thermal hysteresis from our lattice parameters temperature dependence data because the measurements were performed in 5 K steps, but from the magnetic measurements no hysteresis is expected and it is hard to notice any in our lattice parameters data as well. Judging from the small

volume change at the transition temperature (Fig. 6, bottom curve) this transition is weakly first-order, in agreement with heat capacity data.

The crystal structure of sample C (Gd_5Ge_3 prepared using commercial grade Gd) was examined in the temperature range from 295 to 5 K (Figure 8). Similar to A-HT Gd_5Ge_3, it undergoes an orthorhombic distortion at its antiferromagnetic ordering temperature. However, compared with A-HT Gd_5Ge_3 (see Fig. 6) the lattice distortion in C Gd_5Ge_3 is insignificant. Thus, a low resolution temperature dependent diffraction study of the crystal structure of a typical Gd_5Ge_3 sample prepared with impure Gd may not lead to the detection of such a minor distortion (e.g. in a conventional neutron diffraction experiment).

The isothermal increase of magnetic field from 0 to 4 T does not produce any measurable changes in the Gd_5Ge_3 lattice at 20 K (as follows from the least squares standard deviations of lattice parameters listed in Table 3, the sensitivity of our X-ray powder diffraction data is on the order of 20 ppm). The compound remains orthorhombic with practically the same lattice parameters.

It is easy to notice that there are some discrepancies between our data and the earlier reports.[32,33,34] First, no structural distortion was reported by x-ray diffraction study of the magnetic field dependence of the (550) and (008) Bragg reflections performed at 4.2 K. However, because no full-profile and/or temperature dependent study of these reflections has been performed and the transition is already completed at 4.2 K it is likely that no

further structural distortion could be seen in such experiment.[33] It is more difficult to explain the discrepancy between our results and Ref.34. The reported contraction along the *a*-axis[34] may correspond to the contraction along the orthorhombic *b*-axis observed in our study (assuming that the single crystal[34] was oriented at room temperature where *a* and *b* are identical due to hexagonal symmetry). It is difficult to imagine though, that during the hexagonal to orthorhombic transition authors of Ref. 34 obtained a single-domain crystal especially compared to the high probability to form three orthorhombic domains from the original hexagonal crystal. Further, the reported linear expansion along the *c*-axis[34] completely disagrees with our data. Combined with the overall behavior of $\Delta a/a$ and $\Delta c/c$ as functions of temperature reported in Ref. 34, the most reasonable explanation is that the *a* and *c* axes have been switched in that work. Finally, we did not observe the field dependence of the Gd_5Ge_3 lattice parameters at 20 K, while magnetostriction data of Ref. 34 show clear and hysteretic steps along both *a*- and *c*-directions at this temperature. We believe this is due to the magnetocrystalline anisotropy combined with a much higher absolute sensitivity of capacitance dilatometry compared to ~20 ppm accuracy of our x-ray powder diffraction measurements.

THEORETICAL INVESTIGATIONS

In order to have a better insight into the ground state of Gd_5Ge_3, first principles electronic structure calculations have been performed for both experimentally determined orthorhombic (*Cmcm*) and hexagonal ($P6_3/mcm$) structures. The local spin density approximation including Hubbard U parameter (LSDA + U) approach (with $U = 6.7$ eV

and $J = 0.7$ eV – the well-known values for Gd atoms[43]) has been employed within the scalar relativistic version of the tight binding linear muffin tin orbital (TB-LMTO) method.[44] The structural parameters of both crystal structures (lattice constants and atomic positions) were used in these calculations as obtained from X-ray powder diffraction data and were not relaxed.

The spin polarized ferromagnetic (FM) and antiferromagnetic (AFM) total energies of the orthorhombic Gd_5Ge_3 are lower by 16.5 and 192.0 meV/cell compared to the respective FM and AFM total energies of the hexagonal Gd_5Ge_3. For the AFM calculations the orthorhombic and hexagonal symmetries have been converted into the equivalent triclinic structures with P1 symmetry so that each atom in the unit cell is formally no longer equivalent to any other atom in the same unit cell. This facilitated assignment of spins of half Gd atoms in one direction and the other half of Gd atoms in the opposite direction creating AFM configuration.[45] On the other hand, the non-spin polarized paramagnetic (PM) total energy of the hexagonal Gd_5Ge_3 is lower by 19.6 meV/cell compared to the PM total energy of the orthorhombic Gd_5Ge_3. These results confirm that the ground state structure of Gd_5Ge_3 is AFM orthorhombic.

In order to understand how the bands near the Fermi level change during the magnetostructural transformation in Gd_5Ge_3, the PM density of states (DOS) of the fourfold Gd site [Gd1 (4d)] of hexagonal Gd_5Ge_3 is compared with the spin polarized spin up and spin down DOS of the equivalent eightfold Gd site [Gd1 (8e)] of the AFM orthorhombic Gd_5Ge_3 (Fig. 9). The PM bands of Gd1 atoms around the Fermi level split

in spin up and spin down bands by 0.65 eV during the PM hexagonal-AFM orthorhombic transformation. This band splitting causes the imbalance between spin up and spin down integrated DOS up to the Fermi level giving rise to the 5*d* moments on the Gd1 atoms of the AFM orthorhombic Gd_5Ge_3.

While we do not know the exact location of the interstitial impurities in the Gd_5Ge_3 lattice, previous crystallographic studies[46] indicate that the (2b: 0, 0, 0) position of the hexagonal structure may be their preferred location. Therefore, in order to model the influence of such impurities on the ground state of Gd_5Ge_3, we have placed oxygen, nitrogen, and carbon impurities in the interstitial (0, 0, 0) positions of the hexagonal Gd_5Ge_3 and performed the electronic structure calculations. The exchange interactions are estimated by subtracting FM total energy from AFM total energy.[45] As shown in Table 4, the carbon and nitrogen impurities make the exchange interactions more negative indicating stronger antiferromagnetic order and higher T_N. However, oxygen, which is the main impurity in samples prepared using the commercial grade Gd (Table 2), makes exchange interactions slightly less negative, therefore leading to a less stable antiferromagnetic order.

The magnetic moments calculated assuming FM order show that the fourfold Gd1 atoms in the hexagonal Gd_5Ge_3 have higher magnetic moments compared to other Gd atoms (Table 5). Similarly, the eightfold Gd1 (8e) atoms in the orthorhombic Gd_5Ge_3 have highest moments compared to Gd2 (4c) and Gd3 (8g) atoms (Table 5). The Gd moments in the hexagonal structure are reduced when carbon and nitrogen impurities are placed in

the (0,0,0) position of the hexagonal structure. However, the moments of Gd1 atoms are increased but Gd2 are decreased when oxygen impurity is placed in the same interstitial position. This indicates that impurities modify the magnetic moments of non equivalent Gd atoms differently depending on the nature of the impurity atoms. Small but non negligible antiparallel moments obtained for the Ge atoms and impurity atoms are due to the hybridization between the *d* states of Gd atoms and the *p* states of Ge and impurity atoms.

DISCUSSION

The Neél temperature observed in our material (T_N = 87 for sample A-HT) is the highest among those reported in literature. Taking into account that sample A was prepared using the high purity Gd metal from the Ames Laboratory[35], while other studies employed a commercial grade Gd, we postulate that the value of T_N in Gd_5Ge_3 is strongly dependent on the purity of the rare earth metal used in sample preparation. Our second sample made from the high purity Gd (sample B) shows nearly the same T_N = 83 K (see Fig. 4) but sample C made from commercial purity gadolinium has the ordering temperature of 68 K, which is 19 K lower than the first of our samples (Fig. 1b), and in agreement with the Neél temperature reported by Barmin *et al*.[27,28]

Apparently, there are two common mechanisms of how impurities influence the properties of the synthesized Gd_5Ge_3 alloys. The first one involves modification of the crystal and electronic structures when impurity atoms, depending on their nature, either

substitute the main atoms or occupy available interstitial space. Second mechanism is related to the fact that an effective concentration of the main component is lower in the low-purity material compared to the high-purity material, so the alloys prepared from the materials of different purity would have different actual compositions.

In order to examine the influence of both mechanisms on the ordering temperature of Gd_5Ge_3 we: a) performed the chemical analysis of major interstitial impurities in samples A-HT and C; and b) prepared two additional samples [$Gd_{5.02}Ge_3$ (D) and $Gd_{5.1}Ge_3$ (E)] with some additional Gd to see if the shift in composition will affect Neél temperature.

The chemical analysis showed that the concentration of the interstitial impurities (O and N) is significantly higher in sample C than in sample A (Table 2). On the other hand the ordering temperature practically does not change with extra Gd added (66 K for sample D and 69 K for sample E) indicating that the Gd deficiency (second mechanism) is not the main reason for the lower T_N in sample C. Thus, presence of interstitial impurities in Gd_5Ge_3 lattice seems to be the main factor affecting the magnetic ordering temperature in this compound.

It is important to note that the samples prepared from the low-purity Gd have smaller lattice parameters than the samples made from the high-purity Gd (Table 1). It appears that this contradicts our explanations because higher concentration of the interstitial atoms usually translates into larger lattice parameters. However, the structural properties of compounds with the Mn_5Si_3-type structure substantially differ from the majority of

intermetallic systems in this respect. In the Mn_5Si_3 structure the void that surrounds the (2b: 0, 0, 0) position is so large that most of the typical interstitial atoms (B, C, N, O) actually shrink the lattice around them after forming chemical bonds with the neighboring atoms. This effect is well studied in the La_5Ge_3 compound[46] as well as in a few other intermetallic compounds with the Mn_5Si_3 crystal structure.[47,48] The lattice parameters of Gd_5Ge_3 reported by Dhar *et al.*,[31] who also reported a high T_N, are remarkably close to the lattice parameters of our samples A, A-HT and B, while the lattice parameters of the gadolinium germanide with lower T_N reported by Barmin *et al.*[27] are close to those of the low-purity samples C, D, and E.

Thus, it is clear that both the unit cell volume and the magnetic ordering temperature are reduced in Gd_5Ge_3 with high concentrations of interstitial impurities. According to the high pressure magnetization measurements (Fig. 4), the reduction of T_N is not due to the overall unit-cell contraction (i.e., chemical pressure effect) – otherwise the ordering temperature of the pure Gd_5Ge_3 would have decreased when the hydrostatic pressure was applied, while it actually increases. Therefore, such reduction must be a result of chemical interactions between an interstitial element and the parent compound. There is enough evidence to suggest that different interstitial impurities affect T_N in a different way. First of all, this assumption is supported by the first principle calculations (Table 4), which suggest that oxygen (the main impurity in our compounds) reduces the strength of the AFM interactions in the parent Gd_5Ge_3, while both carbon and nitrogen may enhance it. Furthermore, recent work by Wrubl *et al.*[49] presents experimental evidence that in the $Gd_5Ge_3C_{0.33}$ phase the Neel temperature is slightly higher than in the parent Gd_5Ge_3

alloy, even though the lattice parameters and unit cell volume are lower. This indicates that the magnetic properties of the Gd_5Ge_3 are much more sensitive to the particular impurity than they are to the change of the unit cell volume. We note, however, that our calculations overestimate the influence of carbon on the magnetic properties of Gd_5Ge_3,[49] while they probably, underestimate the effect of oxygen, because the actual change of T_N in our oxygen-rich samples is significantly larger than the calculated -3.5 K difference (see Figure 1b and Table 4). No data are available for the nitrogen-rich Gd_5Ge_3 but one can expect that the influence of interstitial nitrogen would be comparable to that of carbon (Table 4).

The results of temperature dependent X-ray powder diffraction experiment indicate that the presence of impurity atoms makes the energy difference between PM and AFM phases smaller resulting in the magnetic ordering transition that may not require a structural change at T_N. Such a prominent effect of the rare earth metals purity on the presence (or absence) of the structural transitions has been earlier observed in Er_5Si_4,[50,51] where the structural transition occurs only in samples prepared with high purity Er.

CONCLUSIONS

The Gd_5Ge_3 compound prepared using high purity Gd exhibits a structural transition at the AFM transition (T_N = 87 K). The low temperature crystal structure is a new orthorhombic type of structure with the space group *Cmcm*. In the sample prepared using low-purity Gd the structural distortion is minor, and the ordering temperature itself is

significantly lower. A few possible spin-reorientation transitions have been observed below T_N at 68 and 44 K, and an additional transition occurs in high magnetic fields above 70 kOe at lower temperatures. The heat capacity peak at T_N remains relatively sharp even in high magnetic fields, which is typical for the first order transitions, but the magnetization and the x-ray powder diffraction measurements indicate the absence of hysteresis and the small volume change at the transition temperature.

The first principles electronic structure calculations confirm that the ground state structure of Gd_5Ge_3 is AFM orthorhombic. The eightfold Gd1 (8e) has the largest magnetic moment compared to the fourfold Gd2 (4c) and eightfold Gd3 (8g) in the orthorhombic Gd_5Ge_3. Nitrogen and carbon impurities enhance the AFM interactions while reducing the spin polarization of 5*d* Gd, but oxygen impurities reduce the AFM interactions and enhance the spin polarization of the 5*d* states of fourfold Gd in Gd_5Ge_3.

Acknowledgements

The Ames Laboratory is operated by Iowa State University of Science and Technology for the U.S. Department of Energy under contract No. DE-AC02-07CH11358. Work at Ames Laboratory is supported by the Office of Basic Energy Sciences, Materials Sciences Division of the Office of Science, U.S. Department of Energy. The authors thank Dr. P. Manfrinetti for valuable comments.

References

[1] V. K. Pecharsky and K. A. Gschneidner, Jr., Pure Appl. Chem. **79**, 1383 (2007), and references therein.

[2] G. J. Miller, Chem. Soc. Rev. **35**, 799 (2006), and references therein.

[3] L. Morellon, J. Stankiewicz, B. Garcia-Landa, P. A. Algarabel, and M. R. Ibarra, Appl. Phys. Lett. **73**, 3462 (1998).

[4] L. Morellon, P. A. Algarabel, M. R. Ibarra, J. Blasco, B. Garcia-Landa, Z. Arnold, and F. Albertini, Phys. Rev. B **58**, R14721 (1998).

[5] E.M. Levin, A.O. Pecharsky, V.K. Pecharsky, and K.A. Gschneidner, Jr., Phys. Rev. B **63**, 064426 (2001).

[6] L. Morellon, P. A. Algarabel, C. Magen, and M. R. Ibarra, J. Magn. Magn. Mater. **237**, 119 (2001).

[7] M. Zou, V. K. Pecharsky, K. A. Gschneidner, Jr., Ya. Mudryk, D. L. Schlagel, and T. A. Lograsso, Phys. Rev. B **80**, 174411 (2009).

[8] V. K. Pecharsky and K. A. Gschneidner, Jr., Phys. Rev. Lett. **78**, 4494 (1997).

[9] V. K. Pecharsky and K. A. Gschneidner, Jr., Appl. Phys. Lett. **70**, 3299 (1997).

[10] V. K. Pecharsky and K. A. Gschneidner, Jr., Adv. Cryo. Eng. **43**, 1729 (1998).

[11] E. M. Levin, V. K. Pecharsky, and K. A. Gschneidner, Jr., Phys. Rev. B **63**, 174110 (2001).

[12] M. Zou, V. K. Pecharsky, K. A. Gschneidner, Jr., D. L. Schlagel, and T. A. Lograsso, J. Alloys Compd. **488**, 550 (2009).

[13] S. B. Roy, M. K. Chattopadhyay, P. Chaddah, J. D. Moore, G. K. Perkins, L. F. Cohen, K. A. Gschneidner, Jr., and V. K. Pecharsky, Phys. Rev. B **74**, 012403 (2006).

[14] S. Velez, J. M. Hernandez, A. Fernandez, F. Macià, C. Magen, P. A. Algarabel, J. Tejada, and E. M. Chudnovsky, Phys. Rev. B **81**, 064437 (2010).

[15] Ya. Mudryk, Y. Lee, T. Vogt, K. A. Gschneidner, Jr., and V. K. Pecharsky, Phys. Rev. B **71**, 174104 (2005).

[16] A. O. Pecharsky, K. A. Gschneidner, Jr., V. K. Pecharsky, and C. E. Schindler, J. Alloys Compd. **338**, 126 (2002).

[17] V. K. Pecharsky and K. A. Gschneidner, Jr., Adv. Mater. **13**, 683 (2001).

[18] V. K. Pecharsky, A. O. Pecharsky, and K. A. Gschneidner, Jr., J. Alloys Compd. **344**, 362 (2002).

[19] O. Ugurlu, L. S. Chumbley, D. L. Schlagel, and T. A. Lograsso, Acta Mater. **54**, 1211 (2006).

[20] L. S. Chumbley, O. Ugurlu, R. W. McCallum, K. W. Dennis, Y. Mudryk, K. A. Gschneidner, Jr, and V. K. Pecharsky, Acta Mater. **56**, 527 (2008).

[21] J. D. Moore, K. Morrison, G. K. Perkins, D. L. Schlagel, T. A. Lograsso, K. A. Gschneidner, Jr., V. K. Pecharsky, and L. F. Cohen, Adv. Mater. **21**, 3780 (2009).

[22] N. C. Baezinger and J. J. Hegenbarth, Acta Cryst. **17**, 620 (1964).

[23] E. I. Gladyshevskii, Zh. Strukt. Khim. **5**, 919 (1964).

[24] K. H. J. Buschow and J. F. Fast, Phys. Status Solidi **21**, 593 (1967).

[25] I. Mayer and I. Shidlovsky, Inorg. Chem. **8**, 1240 (1969).

[26] K. S. V. L. Narasimhan, H. Steinfink, and E. V. Ganapathy, J. Appl. Phys. **40**, 51 (1969).

[27] S. M. Barmin, R. P. Krentsis, P. V. Gel'd, and V. G. Batalin, Fiz. Tverd. Tela **21**, 3174 (1979).

[28] S. M. Barmin, D. A. Emel'yanov, R. P. Krentsis, and P. V. Gel'd, Fiz. Tverd. Tela **22**, 1224 (1980).

[29] N. P. Gorbachuk and A. S. Bolgar, Powd. Metallur. Metal Ceram. **40**, 54 (2001).

[30] F. Canepa, S. Cirafici, and M. Napoletano, J. Alloys Compd. **335**, L1 (2002).

[31] S. K. Dhar, P. Manfrinetti, A. Palenzona, and M. Pani, J. Alloys Compd. **347**, 1 (2002).

[32] T. Tsutaoka, Y. Nishiume, and T. Tokunaga, J. Magn. Magn. Mater. **272-276**, e421 (2004).

[33] Y. Narumi, Y. Tanaka, N. Terada, M. Rotter, K. Katsumata, T. Fukui, M. Iwaki, K. Kindo, H. Toyokawa, A. Tanaka, T. Tsutaoka, T. Ishikawa, and H. Kitamura, J. Phys. Soc. Japan **77**, 053711 (2008).

[34] M. Doerr, M. Rotter, A. Devishvili, A. Stunault, J. J. Perenboom, T. Tsutaoka, A. Tanaka, Y. Narumi, M. Zschintzsch, and M. Loewenhaupt, J. Phys.: Confer. Series **150**, 042025 (2009).

[35] Materials Preparation Center, Ames Laboratory of US DOE, Ames, IA, USA, www.mpc.ameslab.gov.

[36] S. Yu. Dan'kov, A. M. Tishin, V. K. Pecharsky, and K. A. Gschneidner, Jr., Phys. Rev. B **57**, 3478 (1998).

[37] K. A. Gschneidner, Jr., J. Alloys Compd. **193**, 1 (1993).

[38] A. B. Gokhale and G. J. Abbaschian, in *Binary Alloy Phase Diagrams*, **2**nd edition, edited by T. B. Massalski (ASM International, Materials Park, OH, USA, 1990), Vol. **2**, p.1881-1883.

[39] V. K. Pecharsky, J. O. Moorman, and K. A. Gschneidner, Jr., Rev. Sci. Instrum. **68**, 4196 (1997).

[40] A. P. Holm, V. K. Pecharsky, K. A. Gschneidner, Jr., R. Rink, and M. N. Jirmanus, Rev. Sci. Instrum. **75**, 1081 (2004).

[41] *International Tables for Crystallography*, vol. A, edited by Theo Hahn (D. Reidel Publishing Company, Dordrecht, Holland, 1983).

[42] B. Hunter, Rietica-A Visual Rietveld Program, International Union of Crystallography Commission on Powder Diffraction Newsletter No. 20, (Summer, 1998) http://www.rietica.org.

[43] V. I. Anisimov, F. Aryasetiawan, and A. I. Lichtenstein, J. Phys.: Condens. Matter. **9**, 767 (1997).

[44] O. K. Andersen and O. Jepsen, Phys. Rev. Lett. **53**, 2571 (1984).

[45] D. Paudyal, V. K. Pecharsky, and K. A. Gschneidner, Jr., J. Phys.: Condens. Matter **20**, 235235 (2008).

[46] A. M. Guloy and J. D. Corbett, Inorg. Chem. **32**, 3532 (1993).

[47] E. Garcia and J. D. Corbett, Inorg. Chem. **29**, 3274 (1990).

[48] Y. U. Kwon and J. D. Corbett, Chem. Mater. **4**, 1348 (1992).

[49] F. Wrubl, K. V. Shah, D. A. Joshi, P. Manfrinetti, M. Pani, C. Ritter, and S. K. Dhar, J. Alloys Compd. **509**, 6509 (2011).

[50] J. M. Cadogan, D. H. Ryan, Z. Altounian, X. Liu, and I. P. Swainson, J. Appl. Phys. **95**, 7076 (2004).

[51] V. K. Pecharsky, A. O. Pecharsky, Y. Mozharivskyj, K. A. Gschneidner, Jr., and G. J. Miller, Phys. Rev. Lett. **91**, 207205 (2003).

Table 1. The nominal compositions and lattice parameters of prepared alloys.

Alloy	Lattice Parameters		
	a, Å	*c*, Å	*V*, Å^3
Gd_5Ge_3 – A[a]	8.5825(1)	6.4702(1)	412.74(1)
Gd_5Ge_3 – A-HT[a]	8.5812(1)	6.4685(1)	412.51(1)
Gd_5Ge_3 – B[a]	8.5837(2)	6.4712(1)	412.92(1)
Gd_5Ge_3 – C[b]	8.5698(2)	6.4532(1)	410.44(1)
$Gd_{5.02}Ge_3$ – D[b]	8.5678(2)	6.4515(1)	410.13(1)
$Gd_{5.1}Ge_3$ – E[b]	8.5706(2)	6.4577(1)	410.80(1)

[a] prepared from the Ames Laboratory, Materials Preparation Center high purity Gd

[b] prepared from commercial grade Gd

Table 2. Concentration of the oxygen, nitrogen, and carbon impurities (in atomic ppm) in Gd_5Ge_3 samples prepared from the Gd metal of different purity. Values given in parenthesis are in weight ppm.

Element	Ames Laboratory Gd	Commercial Gd
O	1,945 (248)	13,728 (1750)
N	206 (23)	7,629 (851)
C	481 (46)	2,217 (212)

Table 3. The low temperature crystal structure of the Gd_5Ge_3 compound (T = 20 K; space group *Cmcm*, a = 14.8806(3), b = 8.5604(2), c = 6.4388(1) Å; the quality of fit: R_p = 8.53 %, R_{wp} = 11.64 %, R_{Bragg} = 3.87). The isotropic thermal displacement parameters of all atoms were assumed to be the same, employing the overall isotropic thermal displacement approximation.

Atom	Wyckoff position	x	y	z
Gd1	8(e)	0.1675(2)	0	0
Gd2	4(c)	0	0.7437(4)	1/4
Gd3	8(g)	0.1221(1)	0.3774(3)	1/4
Ge1	4(c)	0	0.1013(7)	1/4
Ge2	8(g)	0.3048(3)	0.1979(6)	1/4

Table 4. The differences between antiferromagnetic and ferromagnetic total energies (meV/Gd), which are representative of exchange interactions, of hexagonal Gd_5Ge_3 with and without interstitial impurities. The corresponding calculated $T_N = 1/3 \cdot |J_0|/k_B$ Neél temperatures (K) are listed in parentheses.

Without impurity	With Impurity		
	Oxygen	Nitrogen	Carbon
-22.2 (85.9)	-21.3 (82.4)	-26.5 (102.5)	-26.4 (102.1)

Table 5. Magnetic moments of Gd, Ge, and impurity (C, N or O) atoms of Gd_5Ge_3 determined from spin polarized calculations assuming the ferromagnetic order.

Gd_5Ge_3-Ortho.	Gd1(8e)	Gd2(4c)	Gd3(8g)	Ge1(4c)	Ge2(8g)
	7.29	7.22	7.25	-0.02	-0.02
Gd_5Ge_3-Hex.	Gd1(4d)	Gd2(6g)	Ge(6g)	C/N/O	
Gd_5Ge_3	7.28	7.24	-0.02		
Gd_5Ge_3C	7.21	7.12	0.00	0.00	
Gd_5Ge_3N	7.14	7.09	-0.06	-0.11	
Gd_5Ge_3O	7.30	7.22	-0.06	-0.06	

Figure Captions

FIG 1 (Color online). Magnetization of Gd_5Ge_3 as a function of temperature in applied magnetic fields 1, 20, 40, and 70 kOe (a); comparison of M(T) dependences of two Gd samples: lower curve - prepared with Ames Laboratory Gd, upper curve – with commercial Gd (b).

FIG 2 (Color online). ac magnetic susceptibility of the heat treated (filled circles) and as cast (open squares) Gd_5Ge_3 samples, A-HT and A, respectively.

FIG 3 (Color online). Isothermal magnetization as a function of applied magnetic field for the heat-treated Gd_5Ge_3.

FIG 4 (Color online). M(T) dependences of A-HT Gd_5Ge_3 collected at different applied pressures. The inset shows the area near the T_N.

FIG 5 (Color online). Heat capacity of A-HT Gd_5Ge_3 sample measured in magnetic fields 0, 20, 50, and 75 kOe.

FIG 6 (Color online). Lattice parameters of A-HT Gd_5Ge_3 as a function of temperature.

FIG 7 (Color online). X-ray powder diffraction pattern of A-HT Gd_5Ge_3 (orthorhombic phase) at 20 K (a); comparison of the X-ray powder diffraction patterns of A-HT Gd_5Ge_3 at 50 K (orthorhombic phase) and 100 K (hexagonal phase) in the range of Bragg angles from 21.8 to 25.2 deg. 2θ (b).

FIG 8 (Color online). Lattice parameters of C Gd_5Ge_3 calculated from X-ray powder diffraction data collected as a function of temperature during cooling.

FIG 9 (Color online). The non-spin polarized paramagnetic density of states (DOS) around the Fermi level of four-fold Gd1 (4d) of the hexagonal Gd_5Ge_3 compared with the spin polarized spin up and spin down DOS of the equivalent eight-fold Gd1 (8e) of the AFM orthorhombic Gd_5Ge_3.

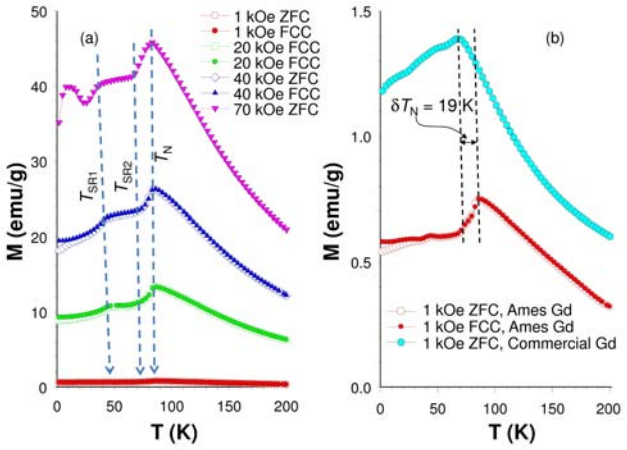

FIG 1 (Color online). Magnetization of Gd_5Ge_3 as a function of temperature in applied magnetic fields 1, 20, 40, and 70 kOe (a); comparison of *M*(T) dependences of two Gd samples: lower curve - prepared with Ames Laboratory Gd, upper curve – with commercial Gd (b).

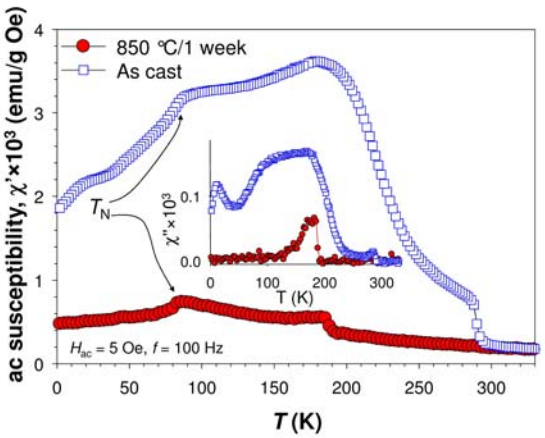

FIG 2 (Color online). ac magnetic susceptibility of the heat treated (filled circles) and as cast (open squares) Gd_5Ge_3 samples, A-HT and A, respectively.

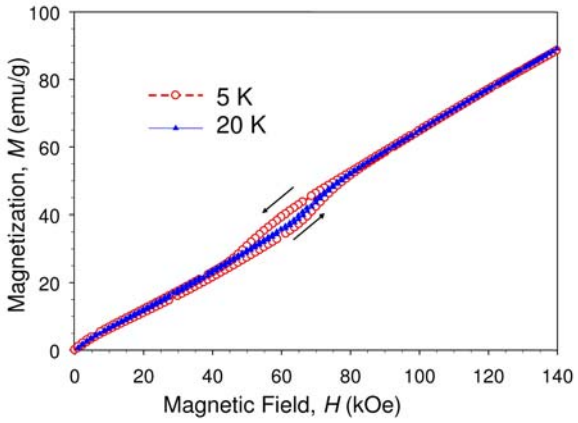

FIG 3 (Color online). Isothermal magnetization as a function of applied magnetic field for the heat-treated Gd_5Ge_3.

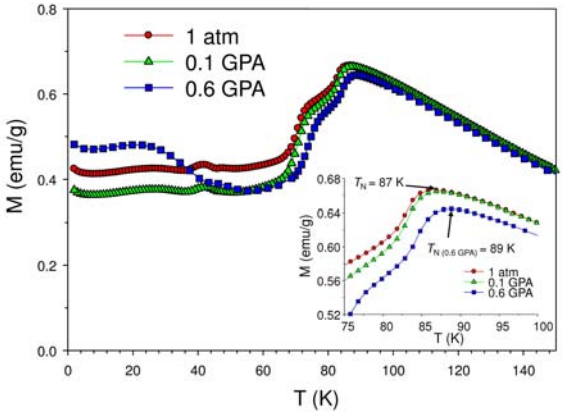

FIG 4 (Color online). *M*(T) dependences of A-HT Gd_5Ge_3 collected at different applied pressures. The inset shows the area near the T_N.

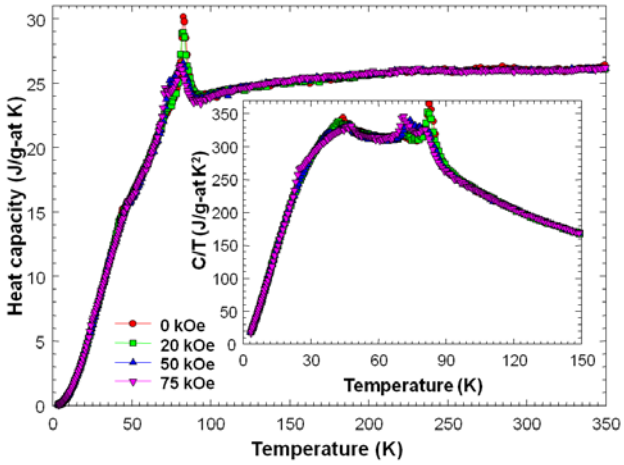

FIG 5 (Color online). Heat capacity of A-HT Gd_5Ge_3 sample measured in magnetic fields 0, 20, 50, and 75 kOe.

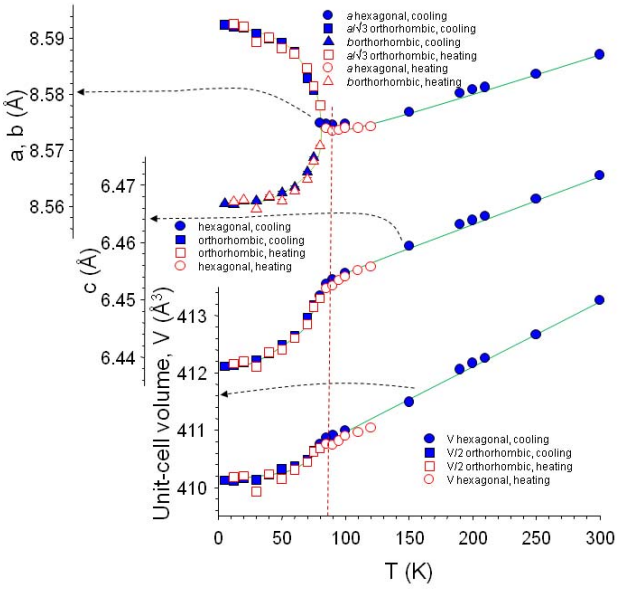

FIG 6 (Color online). Lattice parameters of A-HT Gd_5Ge_3 as a function of temperature.

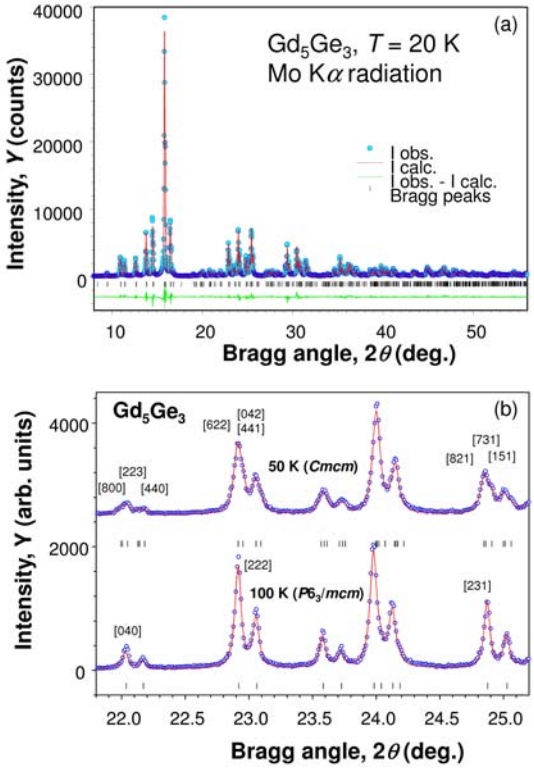

FIG 7 (Color online). X-ray powder diffraction pattern of A-HT Gd_5Ge_3 (orthorhombic phase) at 20 K (a); comparison of the X-ray powder diffraction patterns of A-HT Gd_5Ge_3 at 50 K (orthorhombic phase) and 100 K (hexagonal phase) in the range of Bragg angles from 21.8 to 25.2 deg. 2θ (b).

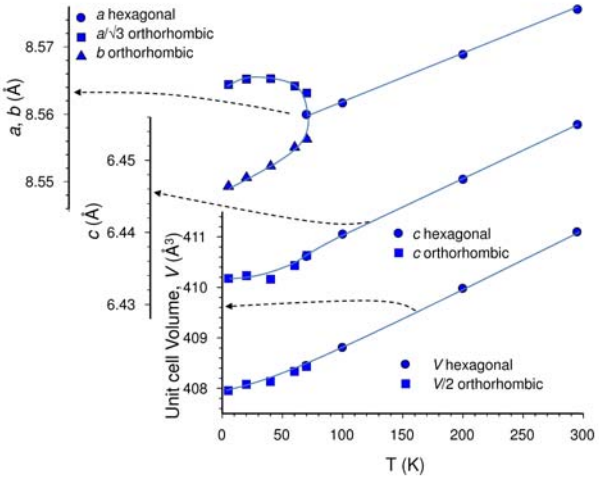

FIG 8 (Color online). Lattice parameters of C Gd_5Ge_3 calculated from X-ray powder diffraction data collected as a function of temperature during cooling.

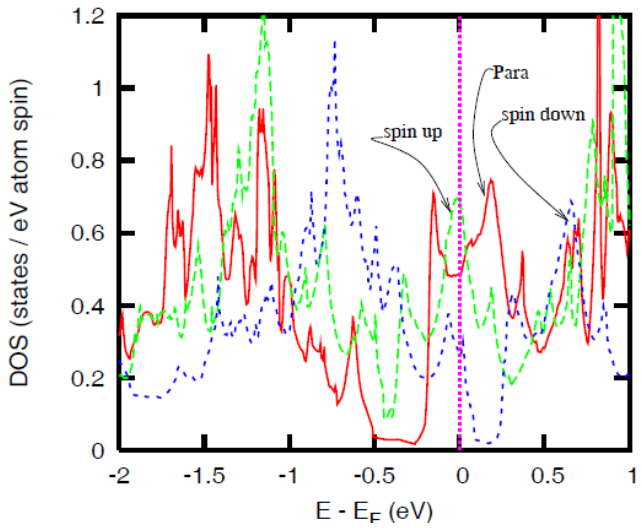

FIG 9 (Color online). The non-spin polarized paramagnetic density of states (DOS) around the Fermi level of fourfold Gd1 (4d) of the hexagonal Gd_5Ge_3 compared with the spin polarized spin up and spin down DOS of the equivalent eightfold Gd1 (8e) of the AFM orthorhombic Gd_5Ge_3.